

# Is there a barrier for the $C_{2v}$ insertion reaction in $O(^1D)+H_2$ ? A test dynamics study based on two-valued energy-switching potential energy surfaces

A.J.C. Varandas<sup>\*</sup>, A.I. Voronin, P.J.S.B. Caridade, A. Riganeli

*Departamento de Química, Universidade de Coimbra, P-3049 Coimbra Codex, Portugal*

Received 25 July 2000; in final form 9 October 2000

## Abstract

We have calculated cross-sections and rate constants for the title reaction by using the quasiclassical trajectory method and a recently reported two-valued energy-switching potential energy surface for the water molecule. By varying the amplitude and rate of decay of a local Gaussian term which controls the appearance of a barrier along the  $C_{2v}$  minimum energy profile, an attempt has been made to answer the title issue. A comparison of the calculated rate constants with the available experimental data suggests that the barrier, if existing, lies below the energy of the reactants, and separates the small van der Waals well from the deep chemical one at short distances. © 2000 Elsevier Science B.V. All rights reserved.

## 1. Introduction

The title reaction plays a fundamental role in combustion chemistry, and is one of the most important in atmospheric chemistry since it leads to hydroxyl radicals which are known to control the upper boundary of the ozone layer. It is therefore not surprising that it has been much studied over the years both theoretically and experimentally. In particular, the reaction dynamics on the ground electronic state potential energy surface has been investigated by both classical trajectory [1–5] and quantum dynamics methods [6–8]. Although it involves in principle five different potential energy surfaces (which correlate with

the electronic states of the reactants), the dominant process is believed to occur on the ground singlet surface  $H_2O(\tilde{X}^1A')$ , at least for low collision energies  $E_{tr} \leq 10$  kJ mol<sup>-1</sup>. This is known to have a deep minimum associated with the stable water molecule which is well characterized from vibrational–rotational spectroscopy [9]. Another aspect of relevance for the title reaction is the fact that it is believed to occur predominantly without an activation barrier and passes via a short lived complex. However, some evidence [10] has been gathered about the possibility that a very small barrier (<10 K or so) may exist along the  $C_{2v}$  path for insertion of  $O(^1D)$  into  $H_2$ . Although the expectations were that such a barrier plays no significant role on the reactivity under thermal and near thermal conditions, a test analysis of this issue has not yet been carried out. Of course, in the absence of an activation barrier, one expects that

<sup>\*</sup> Corresponding author. Fax: +351-239-835-867.

E-mail address: varandas@qtvsl.uc.pt (A.J.C. Varandas).

long range forces play an important role in the dynamics of the title reaction at low translational energies. Thus, in addition to such a conjectured barrier, the potential energy surface must describe properly both the deep well of H<sub>2</sub>O and the subtleties of the O(<sup>1</sup>D)–H<sub>2</sub> long range interaction if one aims to obtain accurate values of the dynamics and kinetics properties for the title reaction.

A two-valued potential energy surface which aims to reach such a level of reliability has recently been proposed by one of the authors [11] using the energy switching [12] (ES) method. It turns out that some recalibration of its parameters has been found [13] to be necessary as it will be further elaborated below. Briefly, this two-valued ES potential energy surface (hereafter referred to as ES-2v I) has been obtained by merging smoothly the realistic Murrell et al. [14] (MCMG) form of the many-body expansion [15] (MBE) type (which has been suitably modified [11] to include long range dispersion forces) with an accurate polynomial-type expansion proposed by Polyanski et al. [16] (which is known to provide a very accurate spectroscopic representation of the potential well). Thus, it will be interesting to use the lowest sheet of the recalibrated two-valued ES potential energy surfaces (labeled ES-2v II and ES-2v III) to carry out test dynamics calculations for the title reaction. We should emphasize that the H<sub>2</sub>O potential energy surface has a multivalued character due to the <sup>1</sup>Σ<sup>-1</sup>Π conical intersection between the two lowest potential energy surfaces of A' (i.e.,  $\tilde{X}^1A'$  and  $\tilde{B}^1A'$ ) and A'' symmetry. In fact, ab initio calculations [14,17,18] even suggest the existence of additional crossings and avoided crossings. In the present work, we have also carried out high-level ab initio calculations of the ground potential energy surface to reveal the possible existence of barriers along the C<sub>2v</sub> and C<sub>∞v</sub> paths.

Although a multistate dynamics study is in principle required to obtain accurate cross-sections and rate constants, it seems warranted to investigate the role of the conjectured potential energy barrier on the dynamics and kinetics of the title reaction under the assumption of electronic adiabaticity. In fact, most O(<sup>1</sup>D) + H<sub>2</sub> dynamics calculations carried out to date have been done under such an assumption, including our own [2]

which have been based on the single-valued ES potential energy surface (ES-SV) of [12]. Moreover, the good agreement between the differential cross-sections obtained from the quasiclassical trajectory (QCT) calculations and the experimentally determined state-resolved ones at low collision energies,  $E_{tr} \leq 10$  kJ mol<sup>-1</sup>, bears witness that the title reaction is consistent with an adiabatic mechanism over a single potential energy surface. Another goal of this work is to discuss the temperature dependence of the rate constant, which is experimentally rather uncertain [19–22]. It should be noted that quantum scattering studies [6–8] indicate that, except for relatively small effects, QCT results should be realistic. We further observe that calculations have also been reported based on multivalued potential energy surfaces, e.g., [23–29].

The structure of the Letter is as follows. In Section 2, we summarize the basic features of the ES-2v I potential energy surface for H<sub>2</sub>O, and its recalibrated forms ES-2v II and ES-2v III. Section 3 provides a description of new ab initio results for the minimum energy paths along C<sub>2v</sub> and C<sub>∞v</sub> geometries. The QCT calculations are reported in Section 4, and discussed in Section 5. Some conclusions are in Section 6.

## 2. Potential energy surfaces

The original two-valued ES potential energy surface for H<sub>2</sub>O (ES-2v I) has been described in detail elsewhere [11], and hence we emphasize here only its major topographical features. Briefly, it reproduces accurately (1 cm<sup>-1</sup> or so) the vibrational levels of the water molecule, and dissociates correctly at all asymptotic channels referring to ground-state H<sub>2</sub>O. In addition, it shows a barrier of a few Kelvin along the minimum energy path for C<sub>2v</sub> insertion of O(<sup>1</sup>D) into H<sub>2</sub>. Such a barrier has been built into the ES-2v I potential energy surface by properly choosing the parameters  $\tilde{B}$  and  $\tilde{b}$  in a local three-body Gaussian term ([11, Eq. (31)]). It has the form

$$V_B = \tilde{B} \exp \left[ -\tilde{b} \sum_{i=1}^3 (R_i - R_i^b)^2 \right], \quad (1)$$

where  $\tilde{B}$  and  $\tilde{b}$  are adjustable parameters, and  $R_i^b$  ( $i = 1$  to 3) defines the location of the barrier. Thus,  $\tilde{B}$  and  $\tilde{b}$  have been originally calibrated [11] from the only requirement that the height of the  $C_{2v}$  insertion barrier should be  $\sim 10$  K and positioned at  $R_1^b = R_2^b = 3.91105a_0$ ,  $R_3^b = 1.42288a_0$ . Since [11] was oriented toward methodological aspects of the ES method, no dynamics study has then been carried out to assert the implications of such a barrier. This is a major goal of the present work.

In the following we focus on two variants of the ES-2v I potential energy surface which have been obtained by recalibrating the parameters  $\tilde{B}$  and  $\tilde{b}$  in Eq. (1) such as to reproduce from QCT calculations the experimental value of the thermal rate constant at  $T = 300$  K [22]:  $k = (1.2 \pm 0.1) \times 10^{-10}$  cm<sup>3</sup> molecule<sup>-1</sup> s<sup>-1</sup>. Since this provides only one piece of input data and there are two adjustable parameters, these have been fixed by looking to other attributes of the fitted surfaces, namely the relative location of the  $C_{2v}$  and  $C_{\infty v}$  curves for O(<sup>1</sup>D) approaching an equilibrium H<sub>2</sub> molecule. The numerical values of the parameters  $\tilde{B}$  and  $\tilde{b}$  are for both of them given in Table 1. Although ES-2v II has been numerically defined in [13], its topographical features will be characterized here in more detail.

Figs. 1 and 2 show the ES-2v II and ES-2v III energy profiles for the  $C_{2v}$  and  $C_{\infty v}$  geometries. Also shown are the ab initio points from our own calculations. As seen from Fig. 1, the ES-2v II potential energy surface displays a small  $C_{2v}$  barrier for insertion of O(<sup>1</sup>D) into H<sub>2</sub> although in contrast to ES-2v I, such a barrier lies now below the classical threshold energy for dissociation. However, as pointed out above and as follows from Fig. 2, their major difference lies in the fact that in the ES-2v III surface the  $C_{\infty v}$  curve for O(<sup>1</sup>D) attacking equilibrium H<sub>2</sub> has a small barrier

Table 1  
Numerical values of the coefficients in Eq. (1) for the ES surfaces

	ES II	ES III
$\tilde{B}/E_h$	-0.01167	-0.009728
$\tilde{b}/a_0^{-2}$	0.264	1.2

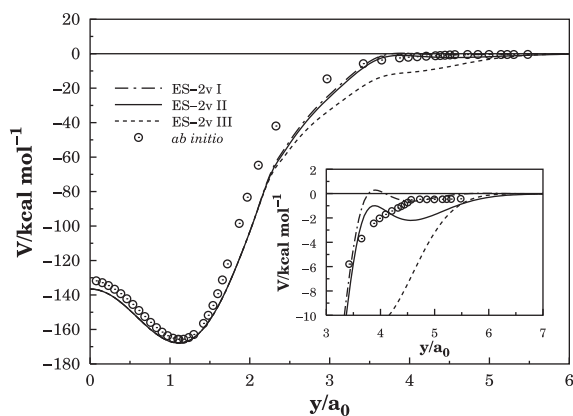


Fig. 1. Energy vs distance plot of the  $C_{2v}$  minimum energy reaction path: ····· ES-2v I; — ES-2v II; - - - ES-2v III. The insert magnifies its long range part.

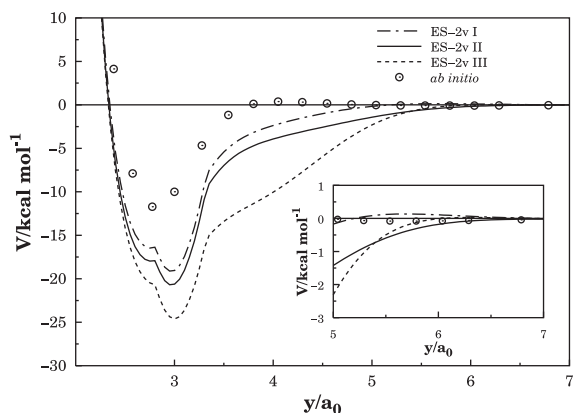


Fig. 2. Same as in Fig. 1 but for the  $C_{\infty v}$  attack of O(<sup>1</sup>D) to H<sub>2</sub> molecule.

and lies above the corresponding curve for  $C_{2v}$  attack. Such a result is in qualitative accord with previous ab initio calculations [30] and our own ones, although there are differences concerning the magnitude and positioning of the barrier crest. Also apparent from these figures is the fact that the ES-2v II potential energy surface is in somewhat better agreement with the ab initio calculations for  $C_{2v}$  geometries than for  $C_{\infty v}$  ones.

At the present time, there are two high quality ab initio surfaces for H<sub>2</sub>O: reproducing kernel Hilbert space interpolation method (RKHS) [1,26]

and Dobbyn and Knowles (DK) [31]. Tests of the accuracy of the ground-state RKHS surface show that such an interpolation is globally good up to 0.3 kcal mol<sup>-1</sup>. It exhibits no barrier for C<sub>2v</sub> geometries but for the C<sub>∞v</sub> reaction path there is a barrier of about 0.7 kcal mol<sup>-1</sup>. Although, the RKHS surface reproduces the experimental reaction exothermicity very well (-1.86 vs -1.84 eV), it underestimates the H<sub>2</sub>O well depth (7.18 vs 7.28 eV). This circumstance could produce some influence on the dynamics of the title reaction. The more recent DK ground-state potential energy surface has been based on calculations employing a larger electronic basis set and reference configurations than those used for the RKHS surface. It is more accurate at least in terms of reproducing the energetics, in particular the H<sub>2</sub>O well depth (7.29 eV). However, their published ab initio points cover only a very restricted region of interatomic distances.

### 3. Ab initio calculations

We have carried out ab initio calculations for both the C<sub>2v</sub> and C<sub>∞v</sub> minimum energy paths. The optimized geometries were obtained at FVCAS level, while energies along the minimum energy paths were calculated at MRCI level including the Davidson correction. The cc-pVQZ and aug-cc-pVQZ basis sets of Dunning [32] have been employed. All calculations were carried out using the MOLPRO package [33], with the results being shown in Figs. 1 and 2. For C<sub>2v</sub> geometries, using

the cc-pVQZ basis set, the calculations predict a small barrier which disappears when using the aug-cc-pVQZ basis set. These results are in good agreement with those of Walch and Harding [30] and Ho et al. [1]. For C<sub>∞v</sub> geometries, an appealing feature is the existence of a small (≈ 0.4 kcal mol<sup>-1</sup>) barrier located at R<sub>HH</sub> = 1.40 a<sub>0</sub>, R<sub>O-HH</sub> = 4.0a<sub>0</sub>, which can be compared with other ab initio data (≈ 0.7 kcal mol<sup>-1</sup>) [1,30]. For the O(<sup>1</sup>D) + H<sub>2</sub>(X<sup>1</sup>Σ<sub>g</sub><sup>+</sup>) dissociation energy, we obtained 7.20 eV which compares with the experimental value of 7.28 eV. Overall, the agreement with the ES surfaces is satisfactory for the C<sub>2v</sub> optimized path. For C<sub>∞v</sub> geometries, the discrepancy is larger but should have little relevance for low energy dynamics especially if a barrier is involved.

### 4. Trajectory calculations

Table 2 provides a summary of the QCT calculations carried out in the present work using the ES-2v II and ES-2v III potential energy surfaces [12] for H<sub>2</sub>O described in Section 2 (the calculations for ES-2v I unreasonably underestimate the rate constant at 300 K, probably due to the presence of a barrier above the dissociation limit for C<sub>2v</sub> geometries, and hence are not given for brevity). Batches of 500 trajectories have been calculated for each of the six translational energies over the range 0.1 ≤ E<sub>tr</sub>/kcal mol<sup>-1</sup> ≤ 12. Note that this number of trajectories is sufficient to yield reactive cross-sections which are typically converged within a few percent. Since the initial rotational quantum

Table 2

A summary of the trajectory calculations: translational energy (kcal mol<sup>-1</sup>), maximum impact parameter (Å), and reactive cross-section (Å<sup>2</sup>)

E <sub>tr</sub>	ES-2v II		ES-2v III	
	b <sub>max</sub>	σ <sup>r</sup> ± Δσ <sup>r</sup>	b <sub>max</sub>	σ <sup>r</sup> ± Δσ <sup>r</sup>
0.1	4.97	54.41 ± 1.59	4.10	32.99 ± 1.14
0.5	4.23	38.40 ± 1.17	4.13	32.01 ± 1.17
2.0	3.70	23.71 ± 0.96	3.44	29.36 ± 0.68
4.0	3.38	16.83 ± 0.80	3.38	30.08 ± 0.59
8.0	2.85	15.03 ± 0.57	3.39	27.09 ± 0.70
12.0	2.54	14.12 ± 0.61	3.07	21.78 ± 0.70

number is believed to play only a minor role in the kinetics of the title reaction, we have fixed it as before [2] at  $j = 1$ .

## 5. Results and discussion

Table 2 shows the calculated cross-sections  $\sigma^r$  which have been fitted to the form

$$\sigma^r = \sigma_{\text{cap}}^r + \sigma_{\text{th}}^r, \quad (2)$$

where  $\sigma_{\text{cap}}^r$  and  $\sigma_{\text{th}}^r$  are the cross-sections associated with a capture-type mechanism and one in which there is a threshold energy for reaction. Thus,

$$\sigma_{\text{cap}}^r = bE_{\text{tr}}^{-m} \quad (3)$$

while to define  $\sigma_{\text{th}}^r$  we have used the form

$$\sigma_{\text{th}}^r = c(E_{\text{tr}} - E_{\text{tr}}^0)^n \exp[-d(E_{\text{tr}} - E_{\text{tr}}^0)], \quad E_{\text{tr}} > E_{\text{tr}}^0, \quad (4)$$

$$\sigma_{\text{th}}^r = 0, \quad E_{\text{tr}} \leq E_{\text{tr}}^0, \quad (5)$$

where  $b$ ,  $c$ ,  $d$ ,  $m$ , and  $n$  are least-squares parameters. Note that the threshold energy  $E_{\text{tr}}^0$  has been taken as zero, and hence there is room for a capture-type mechanism at very low translational energies. Specifically, for the ES-2v II potential energy surface, the absence of a barrier for any approaching direction of the oxygen atom to  $\text{H}_2$  suggests that a physically meaningful fit can be obtained by assuming simply a capture mechanism [34]. Thus,  $\sigma^r \equiv \sigma_{\text{cap}}^r$ , with the calculated least-squares parameters being  $b = 29.9546 \text{ \AA}^2 (\text{kcal mol}^{-1})^m$  and  $m = 0.3132$ . A graphical representation of the resulting fit together with the calculated cross-sections is presented in Fig. 3. In turn, for the ES-2v III surface, the complete form of Eq. (2) is better justified. The adjustable parameters have then been calculated to be  $b = 29.2006 \text{ \AA}^2 (\text{kcal mol}^{-1})^m$ ,  $m = 0.0831$ ,  $c = 0.8173 \text{ \AA}^2 (\text{kcal mol}^{-1})^{-n}$ ,  $d = 0.8129 \text{ kcal}^{-1} \text{ mol}$ , and  $n = 3.5072$ . The calculated cross-sections and fitted curve are also given in Fig. 3. Although the above five-parameter fit rests on the six uncertain numbers of Table 2, we believe that it has no spurious fea-

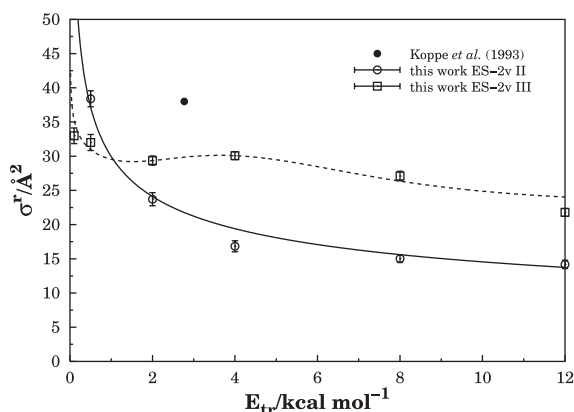


Fig. 3. Cross-sections vs translational energy for the title reaction. Key for symbols:  $\circ$ , this work ES-2v II;  $\square$ , this work ES-2v III;  $\bullet$ , (exp.) [20].

tures. Thus, our calculated cross-sections for ES-2v II and ES-2v III show distinct patterns between each other, although in the case of ES-2v II they look qualitatively similar to those obtained using the single-valued ES potential energy surface [2]. Since both ES potential energy surfaces have the proper long range behavior, we believe that they provide a realistic description of the  $\sigma^r$  at low translational energies for which a capture mechanism should dominate. Of course, this pattern is less apparent in the ES-2v III case, since there are two competing mechanisms at play. However, for ultra-low collisional energies, the molecule has time to reorient as the atom approaches it and hence capture should prevail. Conversely, at high collisional energies, there is no time for the atom to choose the optimum path and an over-barrier type mechanism should be expected since a barrier exists for certain atom-diatom orientations. Additionally, the excited potential energy surfaces  $2^1A'$  and  $1^1A''$  may play some role in the dynamics. Also indicated in Fig. 3 is the experimental global cross-section of Koppe et al. [20] which has been obtained by using ‘superthermal’  $\text{O}(^1D)$  atoms generated by photolysis of  $\text{N}_2\text{O}$  at 193 nm; for a critical assessment, see [2].

Fig. 4 shows the calculated rate constant for the title reaction which is obtained by substituting Eq. (2) in the usual expression for the rate constant:

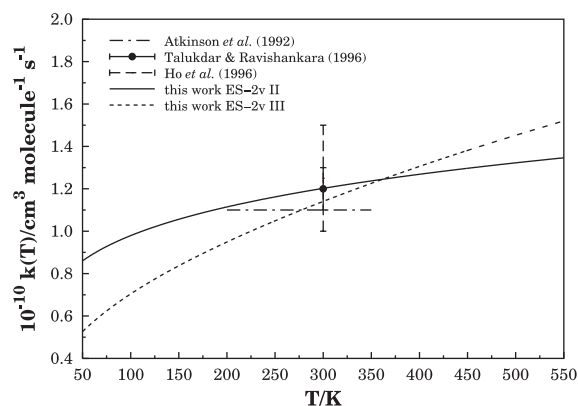


Fig. 4. Rate constant vs temperature for the title reaction. Key for the experimental data: ● and vertical solid error bar, [22]; horizontal dash-dot line, [19]. Also shown by the long-dashed vertical error bar is the recommended [1] error bar at  $T = 298$  K. Key for theoretical data: — ES-2v II; - - - ES-2v III. For further comparisons, the reader is referred to [2] and references therein.

$$\begin{aligned}
 k(T) = & g \left( \frac{8k_B T}{\pi\mu} \right)^{1/2} \left\{ b\Gamma(2-m)(k_B T)^{-m} \right. \\
 & + c \frac{\Gamma(n+1)(k_B T)^n}{(1+dk_B T)^{n+2}} \\
 & \times \left[ (n+1) + \frac{E_{tr}(1+dk_B T)}{k_B T} \right] \\
 & \left. \times \exp \left( -\frac{E_{tr}}{k_B T} \right) \right\}, \quad (6)
 \end{aligned}$$

where  $g = 1/5$  accounts for the electronic degeneracy of  $O(^1D) + H_2(X^1\Sigma_g^+)$ ,  $k_B$  the Boltzmann constant,  $\mu$  the O–H<sub>2</sub> reduced mass, and  $\Gamma(\dots)$  is the gamma function. Also shown in Fig. 4 are previous theoretical [1] and experimental results. These include the measurements by Talukdar et al. [22] and the recommended data by Atkinson et al. [19]; their value is  $1.1 \times 10^{-10} \text{ cm}^3 \text{ molecule}^{-1} \text{ s}^{-1}$ , with a reliability of  $\Delta \log k = \pm 0.1$  at 298 K. Although not strictly comparable with our thermalized results (see [2]), we also mention the absolute nonthermal rate constant ( $2.7 \pm 0.6 \times 10^{-10} \text{ cm}^3 \text{ molecule}^{-1} \text{ s}^{-1}$ ) reported by Koppe et al. [20]. Moreover, we identify in Fig. 4 by a vertical error bar the range  $1.2\text{--}1.3 \pm 0.2 \times 10^{-10} \text{ cm}^3 \text{ molecule}^{-1} \text{ s}^{-1}$ ; this falls over the value reported by Talukdar et al. [22], and has been suggested by Ho et al. [1] to

encompass the best estimates for  $k(T=300 \text{ K})$ . For clarity, all error bars referring to the other data have been omitted. The notable feature from Fig. 4 is therefore the fact that our recalibrated ES-2v surfaces reproduce the best available experimental value at 300 K but show somewhat different rates of increase as a function of temperature. The rate constant for the ES-2v III surface shows a more strong temperature dependence than that obtained with the ES-2v II surface. This is due to the second contribution in Eq. (6) which accounts for the over-barrier mechanism. For further comparisons, the reader is referred to [2].

Our results seem also to indirectly support that for low energies ( $E_{tr} \leq 10 \text{ kJ mol}^{-1}$ ) the prevalent mechanism for reaction is through  $C_{2v}$  insertion of  $O(^1D)$  into  $H_2$  rather than by abstraction. However, at higher energies, recent cross-molecular beam experiments by Che and Liu [35] and trajectory studies [1,23,26] suggest that it is likely that more than one reaction pathway is involved. We further observe that existence of a barrier for reaction is incompatible (at least at the classical level of dynamics) with a capture-type mechanism at low energies. This seems also incompatible with the measured weak temperature dependence of  $k(T)$ . From the theoretical point of view, the relative positioning of the  $C_{\infty v}$  and  $C_{2v}$  curves for the ES-2v II potential energy surface seem to conflict with the ab initio energies of Walch and Harding [30] and ours, which favor ES-2v III. Note that the Walch and Harding [30] and our own calculations show the  $C_{\infty v}$  curve lying above the  $C_{2v}$  energy profile, with the former displaying a small barrier at relatively short distances. However, such a barrier is absent in the ab initio calculations of Li et al. [10], which show instead a small minimum for  $C_{\infty v}$  geometries at  $R \sim 6.2a_0$ . Thus, the fact the energy barrier along the  $C_{\infty v}$  curve of ES-2v III is only  $0.1 \text{ kcal mol}^{-1}$  and appears earlier in the entrance channel seems to provide a realistic compromise between the ab initio predictions. Given the above uncertainty about the most favorable reaction path, and the fact that the dynamics may finally require the inclusion of quantum effects (including nonadiabatic ones), it is difficult to say which ES potential energy surface should be preferred. Since ES-2v II shows a flatter variation of

$k(T)$  vs  $T$  in accordance with the recommended data it is probably more reliable for dynamics and kinetics studies.

## 6. Conclusions

The QCT calculations reported in this work using two variants of a recently proposed two-valued ES H<sub>2</sub>O potential energy surface [12] have been shown to provide an excellent representation of the O(<sup>1</sup>D)+H<sub>2</sub> rate constant at room temperature. This was achieved by slightly decreasing the tiny barrier located along the C<sub>2v</sub> insertion path such that its crest lied below the classical energy of the reactants. We conjecture that this fact may still be compatible with the recent observation [1] that O(<sup>1</sup>D) atoms may not react with H<sub>2</sub> at ultra-low temperatures. In fact, an answer to this must take into account any possibility of vibrational stabilization due to differences in zero-point energy at the reactants and at the barrier. In [1], it is proposed an alternative explanation for the absence of reactivity taking into account many-body effects. Clearly, quantum dynamics calculations would be welcome to test our hypothesis. A more detailed dynamics study by looking to subtle attributes such as differential cross-sections and vector properties would also be useful. Moreover, high level ab initio calculations could help to clarify the issue concerning the relative positioning of the C<sub>2v</sub> and C<sub>∞v</sub> energy profiles discussed in the text.

## Acknowledgements

This work has the support of Fundação para a Ciência e Tecnologia, Portugal, under programme PRAXIS XXI.

## References

- [1] T.-S. Ho, T. Hollebeek, H. Rabitz, L.B. Harding, G.C. Schatz, *J. Chem. Phys.* 105 (1996) 10472.
- [2] A.J.C. Varandas, A.I. Voronin, A. Riganelli, P.J.S.B. Caridade, *Chem. Phys. Lett.* 278 (1997) 325.
- [3] A.J. Alexander, F.J. Aoiz, L. Bañares, M. Brouard, V.J. Herrero, J.P. Simons, *Chem. Phys. Lett.* 278 (1997) 313.
- [4] F.J. Aoiz, *Faraday Discuss.* 110 (1998) 245.
- [5] F.J. Aoiz, L. Bañares, V.J. Herrero, *J. Chem. Soc., Faraday Trans.* 94 (1998) 2483.
- [6] J. Dai, *J. Chem. Phys.* 107 (1997) 4934.
- [7] G.G. Balint-Kurti, A.I. Gonzalez, E.M. Goldfield, S.K. Gray, *Faraday Discuss.* 110 (1998) 169.
- [8] S.K. Gray, E.M. Goldfield, G.C. Schatz, G.G. Balint-Kurti, *Phys. Chem. Chem. Phys.* 1 (1999) 1141.
- [9] H.Y. Mussa, J. Tennyson, *J. Chem. Phys.* 109 (1998) 10885.
- [10] Z. Li, V.A. Apkarian, L.B. Harding, *J. Chem. Phys.* 106 (1997) 942.
- [11] A.J.C. Varandas, *J. Chem. Phys.* 107 (1997) 867.
- [12] A.J.C. Varandas, *J. Chem. Phys.* 105 (1996) 3524.
- [13] A.J.C. Varandas, A.I. Voronin, P.J.S.B. Caridade, *J. Chem. Phys.* 108 (1998) 7623.
- [14] J.N. Murrell, S. Carter, I.M. Mills, M.F. Guest, *Mol. Phys.* 42 (1981) 605.
- [15] J.N. Murrell, S. Carter, S.C. Farantos, P. Huxley, A.J.C. Varandas, *Molecular Potential Energy Functions*, Wiley, Chichester, 1984.
- [16] O.L. Polyanski, P. Jensen, J. Tennyson, *J. Chem. Phys.* 105 (1996) 6490.
- [17] G. Durant, X. Chapuisat, *Chem. Phys.* 96 (1985) 381.
- [18] F. Schneider, F. Di Giacomo, F.A. Gianturco, *J. Chem. Phys.* 104 (1996) 5153.
- [19] R. Atkinson, D.L. Baulch, R.A. Cox, R.F. Hampson Jr., J.A. Kerr, J. Troe, *J. Phys. Chem. Ref. Data* 21 (1992) 1125.
- [20] S. Koppe, T. Laurent, P.D. Naik, H.-R. Volpp, J. Wolfrum, T. Arusi-Parpar, I. Bar, S. Rosenwaks, *Chem. Phys. Lett.* 214 (1993) 546.
- [21] T. Laurent, P.D. Naik, H.-R. Volpp, J. Wolfrum, T. Arusi-Parpar, I. Bar, S. Rosenwaks, *Chem. Phys. Lett.* 236 (1995) 343.
- [22] R.K. Talukdar, A.R. Ravishankara, *Chem. Phys. Lett.* 253 (1996) 177.
- [23] G.C. Schatz, L.A. Pederson, P.J. Kuntz, *Faraday Discuss.* 108 (1997) 357.
- [24] A.J. Alexander, F.J. Aoiz, L. Bañares, M. Brouard, J.P. Simons, *Phys. Chem. Chem. Phys.* 2 (2000) 571.
- [25] K. Drucker, G.C. Schatz, *J. Chem. Phys.* 111 (1999) 2451.
- [26] G.C. Schatz, A. Papaionou, L.A. Pederson, L.B. Harding, T. Hollebeek, T.-S. Ho, H. Rabitz, *J. Chem. Phys.* 107 (1997) 2340.
- [27] F.J. Aoiz, L. Bañares, V.J. Herrero, *Chem. Phys. Lett.* 310 (1999) 277.
- [28] Y.-T. Hsu, K. Liu, L.A. Pederson, G.C. Schatz, *J. Chem. Phys.* 111 (1999) 7921.
- [29] Y.-T. Hsu, K. Liu, L.A. Pederson, G.C. Schatz, *J. Chem. Phys.* 111 (1999) 7931.
- [30] S.P. Walch, L. Harding, *J. Chem. Phys.* 88 (1988) 7653.
- [31] A.J. Doblyn, P.J. Knowles, *Mol. Phys.* 91 (1997) 1107.
- [32] T.H. Dunning, *J. Chem. Phys.* 99 (1993) 9790.

- [33] H.-J. Werner, P.J. Knowles, MOLPRO is a package of ab initio programs written by H.-J. Werner, P.J. Knowles, with contributions from J. Almlöf, R.D. Amos, M.J.O. Deegan, S.T. Elbert, C. Hampel, W. Meyer, K.A. Peterson, R. Pitzer, A.J. Stone, P.R. Taylor, R. Lindh, 1998.
- [34] A.J.C. Varandas, in: A.S. Feliciano, M. Grande, J. Casado (Eds.), *Conferencias Plenarias de la XXIII Reunión Bienal de Química*, Universidad de Salamanca, Salamanca, 1991, p. 321.
- [35] D.-C. Che, K. Liu, *J. Chem. Phys.* 103 (1995) 5164.